Dead Cells Induce Innate Anergy via Mertk after Acute Viral Infection

Graphical Abstract
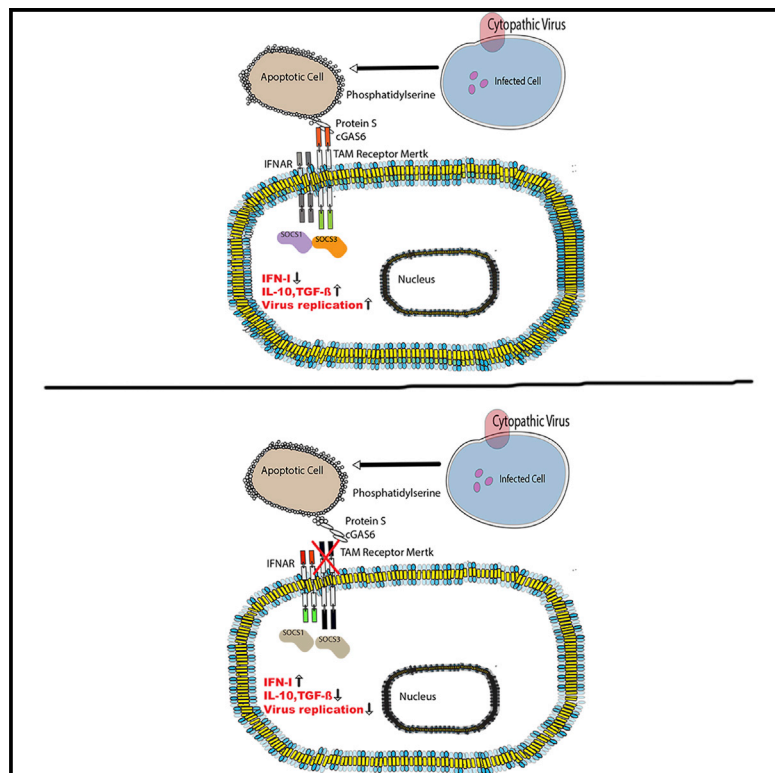
Authors

Tom Adomati, Lamin B. Cham,
Thamer A. Hamdan, ..., Cornelia Hardt,
Philipp A. Lang, Karl S. Lang

Correspondence

wennatom@yahoo.com (T.A.),
karlsebastian.lang@uk-essen.de (K.S.L.)

In Brief

Adomati et al. show that the cytopathic virus VSV leads to innate immune cell anergy. Innate anergy is associated with apoptotic cells through activation of the TAM receptor Mertk and induction of the cytokines IL-10 and TGF-β.

Highlights

- Infection with cytopathic virus, such as VSV, leads to innate anergy

- Innate anergy is associated with apoptotic cells, which activate TAM receptor Mertk

- Mertk signaling induces higher levels of IL-10 and TGF-β and enhances virus replication

- Dexamethasone treatment upregulates Mertk, thereby enhancing innate anergy

CellPress

Dead Cells Induce Innate Anergy via Mertk after Acute Viral Infection

Tom Adomati,[1,10,*] Lamin B. Cham,[1] Thamer A. Hamdan,[1] Hilal Bhat,[1] Vikas Duhan,[1,2] Fanghui Li,[1] Murtaza Ali,[1] Elisabeth Lang,[3] Anfei Huang,[4] Eyad Naser,[5] Vishal Khairnar,[1,6] Sarah-Kim Friedrich,[1] Judith Lang,[1] Justa Friebus-Kardash,[1] Michael Bergerhausen,[1] Maximilian Schiller,[1] Yara Maria Machlah,[1] Florian Lang,[7] Dieter Häussinger,[8] Stanislav Ferencik,[1] Cornelia Hardt,[1] Philipp A. Lang,[4,9] and Karl S. Lang[1,9,*]

[1]Institute of Immunology, University of Duisburg-Essen, Essen, Germany
[2]Immunology in Cancer and Infection Laboratory, QIMR Berghofer Medical Research Institute, Brisbane, QLD, Australia
[3]University Psychiatric Clinics Basel, Basel, Switzerland
[4]Institute of Molecular Medicine, Heinrich Heine University, Düsseldorf, Germany
[5]Department of Molecular Biology, University of Duisburg-Essen, Essen, Germany
[6]Department of Systems Biology, City of Hope Comprehensive Cancer Center, Monrovia, CA, USA
[7]Department of Physiology I, Eberhard Karls University of Tübingen, Tübingen, Germany
[8]Clinic of Gastroenterology, Hepatology and Infectious Diseases, Heinrich Heine University, Düsseldorf, Germany
[9]These authors contributed equally
[10]Lead Contact
*Correspondence: wennatom@yahoo.com (T.A.), karlsebastian.lang@uk-essen.de (K.S.L.)
 https://doi.org/10.1016/j.celrep.2020.02.101

SUMMARY

Infections can result in a temporarily restricted unresponsiveness of the innate immune response, thereby limiting pathogen control. Mechanisms of such unresponsiveness are well studied in lipopolysaccharide tolerance; however, whether mechanisms of tolerance limit innate immunity during virus infection remains unknown. Here, we find that infection with the highly cytopathic vesicular stomatitis virus (VSV) leads to innate anergy for several days. Innate anergy is associated with induction of apoptotic cells, which activates the Tyro3, Axl, and Mertk (TAM) receptor Mertk and induces high levels of interleukin-10 (IL-10) and transforming growth factor β (TGF-β). Lack of Mertk in $Mertk^{-/-}$ mice prevents induction of IL-10 and TGF-β, resulting in abrogation of innate anergy. Innate anergy is associated with enhanced VSV replication and poor survival after infection. Mechanistically, Mertk signaling upregulates suppressor of cytokine signaling 1 (SOCS1) and SOCS3. Dexamethasone treatment upregulates Mertk and enhances innate anergy in a Mertk-dependent manner. In conclusion, we identify Mertk as one major regulator of innate tolerance during infection with VSV.

INTRODUCTION

During viral infections, cell death via apoptosis is a common phenomenon (Roulston et al., 1999). A number of diseases are associated with increased apoptosis, such as infections induced by Ebola virus or human immunodeficiency virus 1 (HIV-1)

(Kaminskyy and Zhivotovsky, 2010). The nature of cell death was proposed to influence the type of immune response. Apoptotic cell death is a "silent death" and is tolerogenic, whereas necrosis is a "violent death" that releases a number of immunostimulatory molecules (Green et al., 2009; Voll et al., 1997; Byrne and Reen, 2002; Zhang and Zheng, 2005). Recognition of apoptotic cells by phagocytes can lead to induction of transforming growth factor β (TGF-β) and interleukin-10 (IL-10), a potent immunosuppressant that contributes to the establishment of a local immunosuppressive milieu (Zhang and Zheng, 2005; Chen et al., 2001).

Apoptosis is mediated by the activation of members of the caspase family of proteases (Taylor et al., 2008; Fuchs and Steller, 2011). Caspase-3, an effector caspase, functions primarily to cause the morphological features of apoptosis (Hunter et al., 2007). The hallmarks of apoptotic cell death are plasma membrane blebbing, cell shrinkage, and the loss of membrane phosphatidylserine (PS) symmetry. The exposure of PS on the outer leaflet of the cytoplasmic membrane is recognized by phagocytic PS receptors, integrins ($\alpha_v\beta_3$ and $\alpha_v\beta_5$), scavenger receptor CD36, and the Mertk receptor tyrosine kinase through association with secreted PS-binding proteins, such as protein S1 (PROS1), growth arrest specific 6 (GAS6), and milk fat globule-epidermal growth factor 8 (MFG-E8) on apoptotic cell surfaces (Erwig and Henson, 2008; Hanayama et al., 2002; Nakano et al., 1997).

Mertk belongs to the TAM (Tyro3, Axl, and Mertk) RTK family, which is normally expressed by macrophages, dendritic cells (DCs), and natural killer cells (Verma et al., 2011). These receptors are known to quench host innate immune responses after engaging their ligands GAS6 and PROS1, which recognize PS on apoptotic cells (Lemke and Rothlin, 2008). TAM receptor ligands are also expressed variably by a number of immune cells, including macrophages, DCs, and activated T cells (Seitz et al., 2007; Nassar et al., 2017; Carrera Silva et al., 2013). This mechanistically linked actions of TAM receptors on macrophages or

DCs activates a negative feedback loop that tempers the innate immune responses initiated by Toll-like receptor (TLR) and type I interferon (IFN-I) signaling pathways (Behrens et al., 2003). TAM receptor signaling is associated with inhibition of the production of proinflammatory cytokines, such as tumor necrosis factor (TNF)-α, IL-6, IL-12, and IFN-I, and with induction of inhibitory gene expression, most prominently the suppressor of cytokine signaling (SOCS) proteins 1 and 3 (SOCS1 and SOCS3) (Rothlin et al., 2007).

During bacterial infection, lipopolysaccharide (LPS) tolerance is a homeostatic mechanism essential for limiting the innate response to endotoxin, thereby reducing host damage and promoting the resolution of inflammation. LPS tolerance is associated with a sharp reduction in the expression of proinflammatory cytokines, such as TNF-α, IL-10, and IL-6, in response to LPS stimulation (Biswas and Lopez-Collazo, 2009; Medvedev et al., 2006). However, what is still unknown is whether cytopathic viruses, such as vesicular stomatitis virus (VSV), can induce tolerogenic mechanisms similar to those associated with LPS tolerance to maintain homeostasis. We postulated that infection with VSV results in the induction of cell death via apoptosis, and the exposed PS on the virus-infected cells becomes coated with the ligands and acts as a potent Mertk agonist, which triggers Mertk signaling and thus limits the innate response. The failure to mount a full immune response against target cells due to immune regulatory mechanisms evoked by virus-induced dead cells results in a state of anergy. We identified Mertk as an important mediator of innate tolerance during infection with VSV.

RESULTS

Infection with VSV Induces Innate Anergy

To test whether viral infection can induce innate unresponsiveness, we infected C57BL/6 wild-type (WT) mice with 2×10^8 plaque-forming units (PFUs) of VSV. Control mice were left uninfected (naive). Next, 48 h later, we challenged both groups with polyinosinic:polycytidylic acid (poly [I:C]) and determined serum IFNα levels at indicated time points. As expected, challenge of naive mice with either VSV or poly (I:C) induced a robust systemic IFNα response (Figure 1A). However, mice that were first challenged with VSV and then with poly (I:C) did not produce systemically measurable IFNα levels (Figure 1A). VSV is a highly cytopathic virus, which typically kills target cells a few hours after infection (Gaddy and Lyles, 2005). Because it has been shown that dead cells can suppress immune activation, we postulated that dead cells may contribute to innate unresponsiveness during VSV infection. To test this hypothesis, we analyzed active caspase-3 in spleens 0, 2, 8, and 24 h after VSV infection. Only spleens of VSV-infected mice exhibited strongly enhanced numbers of apoptotic cells, as demonstrated by detectable levels of active caspase-3 (Figure 1B). Next, we analyzed the splenocytes from naive and VSV-infected WT mice by fluorescence-activated cell sorting (FACS) to determine whether these cells are apoptotic. We detected enhanced frequencies of annexin V+ splenocytes in VSV-infected mice when compared to naive control mice (Figure 1C). Some of these cells were additionally positive for 7-amino-actinomycin D (7-AAD) (Figure 1C). These data suggest that VSV infection induces PS exposure and

apoptosis early after infection. VSV is known to infect a wide range of cell types, indicating that the receptor target(s) for glycosylated (G) protein are commonly expressed molecules (Barber, 2005; Rose, 2001). Further investigation of the source of dead cells revealed that hematopoietic and non-hematopoietic stromal cells activated caspase-3 during VSV infection (Figure 1D). Because VSV is very sensitive to IFN-I-mediated innate immune defenses, we anticipated that a deficiency in the IFN-I receptor and TLR signaling pathways would lead to increased VSV replication and thereby enhance cell death. Indeed, spleens of *Ifnar*−/− and *Myd88/Trif/Cardif*−/− mice showed substantially increased numbers of apoptotic cells compared to WT control spleens after VSV infection (Figure 1E). In line, frequencies of PS exposing splenocytes was increased in VSV-infected *Ifnar*−/− and *Myd88/Trif/Cardif*−/− mice (Figure S1A). DCs are known to play key roles in initiating immune response and in inducing immunological tolerance, depending on their maturation state and subsets (Zhang et al., 2004; Svensson et al., 2004; Wakkach et al., 2003). On the basis of the above findings, we proposed that the dead cells may activate inhibitory signals during VSV infection and that this signal reduces IFN-I induction. In fact, pretreatment of bone-marrow-derived DCs (BMDCs) harvested from WT mice with dead B16F10 cells significantly blunted *Ifna4* induction after challenge with ultraviolet (UV) inactivated VSV (UV-VSV), VSV, or poly(I:C) (Figures 1F and 1G). These findings indicated that dead cells limit IFNα induction and IFNα anergy is associated with apoptotic cells *in vivo*.

Dead Cells Induce Innate Anergy via Mertk

Mertk is a member of the TAM family and has been shown to regulate the innate immune response to apoptotic cells by inhibiting DC activation in animal models (Wallet et al., 2008). Apoptotic cells were also shown to induce the expression of Mertk (A-Gonzalez et al., 2009). Based on these findings, we speculated that Mertk signaling may be involved in innate anergy after acute viral infection. To test this theory, we investigated the Mertk expression profile in the immune cells of naive mice. FACS analysis of the splenocytes revealed strong expression of Mertk by macrophages and DCs (Figure 2A). Both cell types are known to be involved in the induction of IFN-I. Other immune cells tested showed limited or no expression of Mertk (Figure 2A). *In vitro*, naive bone-marrow-derived macrophages (BMDMs) and BMDCs express high levels of Mertk (Figure 2B). DCs are one of the strong producers of IFN-I, and we wondered whether Mertk signaling could influence IFN-I induction in DCs during viral infection. We infected BMDCs generated from *Mertk*−/− or littermate WT control mice (*Mertk*+/+) with VSV and analyzed the mRNA for IFN-I induction. BMDCs from *Mertk*−/− mice showed strong expression of *Ifna4* and *Ifnb1* when compared to those from *Mertk*+/+ mice (Figure 2C). Moreover, the inflammatory cytokines *Tnfa5* and *Il6* were significantly enhanced in *Mertk*−/− BMDCs when compared to *Mertk*+/+ BMDCs (Figure 2C). In line, IFNα protein level from the supernatants of *Mertk*−/− BMDCs were enhanced when compared to *Mertk*+/+ BMDCs (Figure S2A). *In vivo*, spleens of VSV-infected *Mertk*−/− mice showed accelerated *Ifna4* and *Ifnb1* mRNA induction when compared to *Mertk*+/+ mice (Figure 2D). Similarly, *Tnfa5* and *Il6* was higher in spleens of *Mertk*−/− mice (Figure 2D).
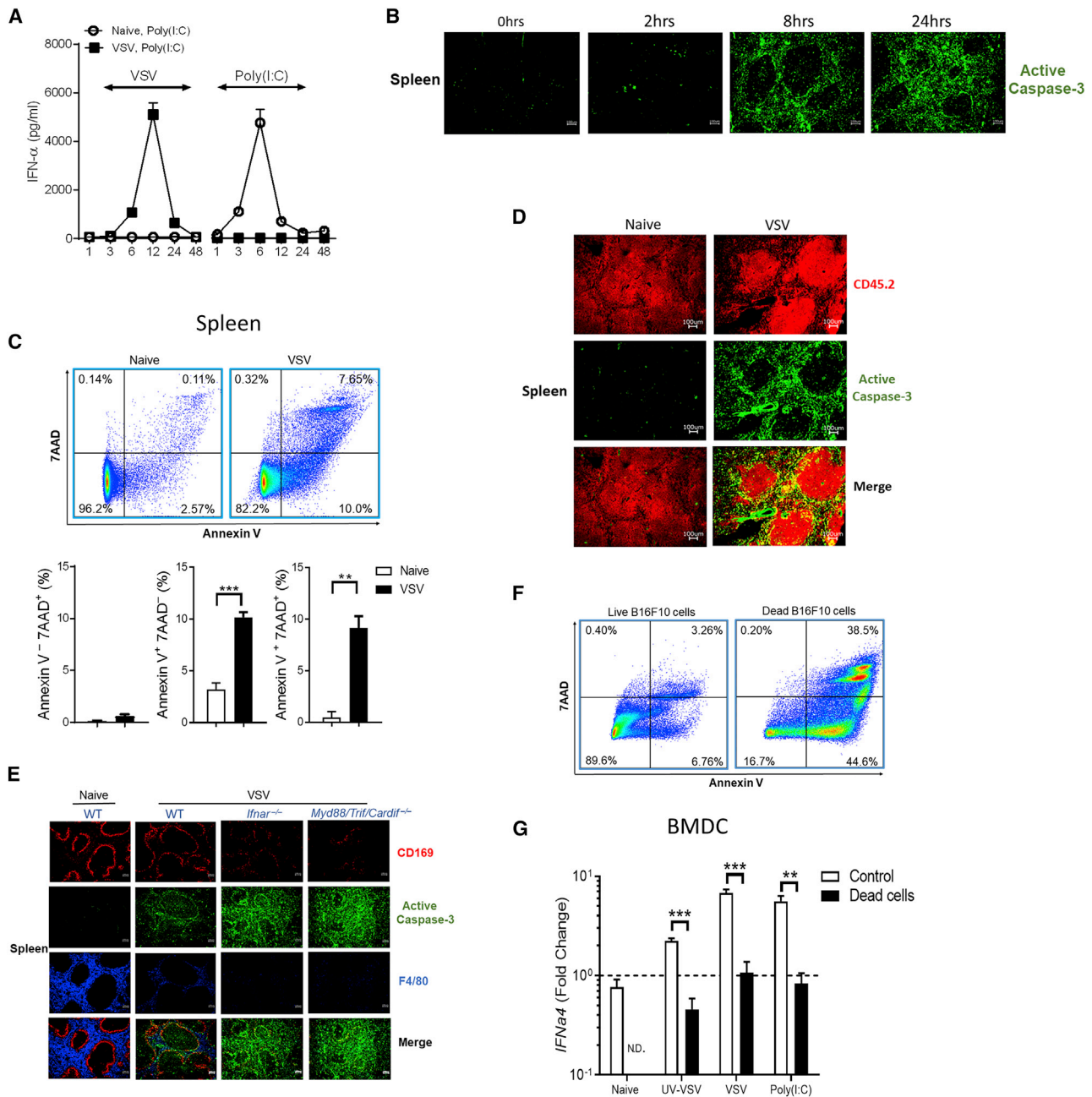
Figure 1. Infection with Vesicular Stomatitis Virus Induces Innate Anergy

(A) IFNα in naive WT mice or mice infected with 2×10^8 PFU VSV intravenously (i.v.) and 48 h later, challenged intraperitoneally (i.p.) with poly (I:C) (50 μg/mouse; n = 3).

(B) Spleens of WT mice infected with 2×10^8 PFU VSV i.v. and stained for active caspase-3 (green; n = 4).

(C) FACS of splenocytes for 7AAD and annexin V of naive WT mice or WT mice immunized with 2×10^8 PFU VSV i.v. (8 h; n = 3).

(D) Spleens of naive WT mice or mice infected with 2×10^8 PFU VSV i.v. (8 h) and stained for active caspase-3 (green) and CD45.2 (red; n = 4).

(E) Spleens of naive WT mice or WT, *Ifnar*$^{-/-}$, and *Myd88/Trif/Cardif*$^{-/-}$ mice infected with 2×10^8 PFU VSV i.v. (8 h) and stained for CD169 (red), active caspase-3 (green), and F4/80 (blue; n = 3).

(F) FACS of B16F10 cells for apoptosis.

(G) *IFNα4* mRNA in BMDCs of WT mice that were left naive or pretreated with apoptotic B16F10 cells or media and then treated with UV-VSV (MOI1), VSV (MOI1), or poly (I:C) (10 μg/mL; n = 3). All data are shown as mean +/- SEM. *p < 0.05; **p < 0.01; ***p < 0.001; ****p < 0.0001 (Student's t test). ns = not significant.
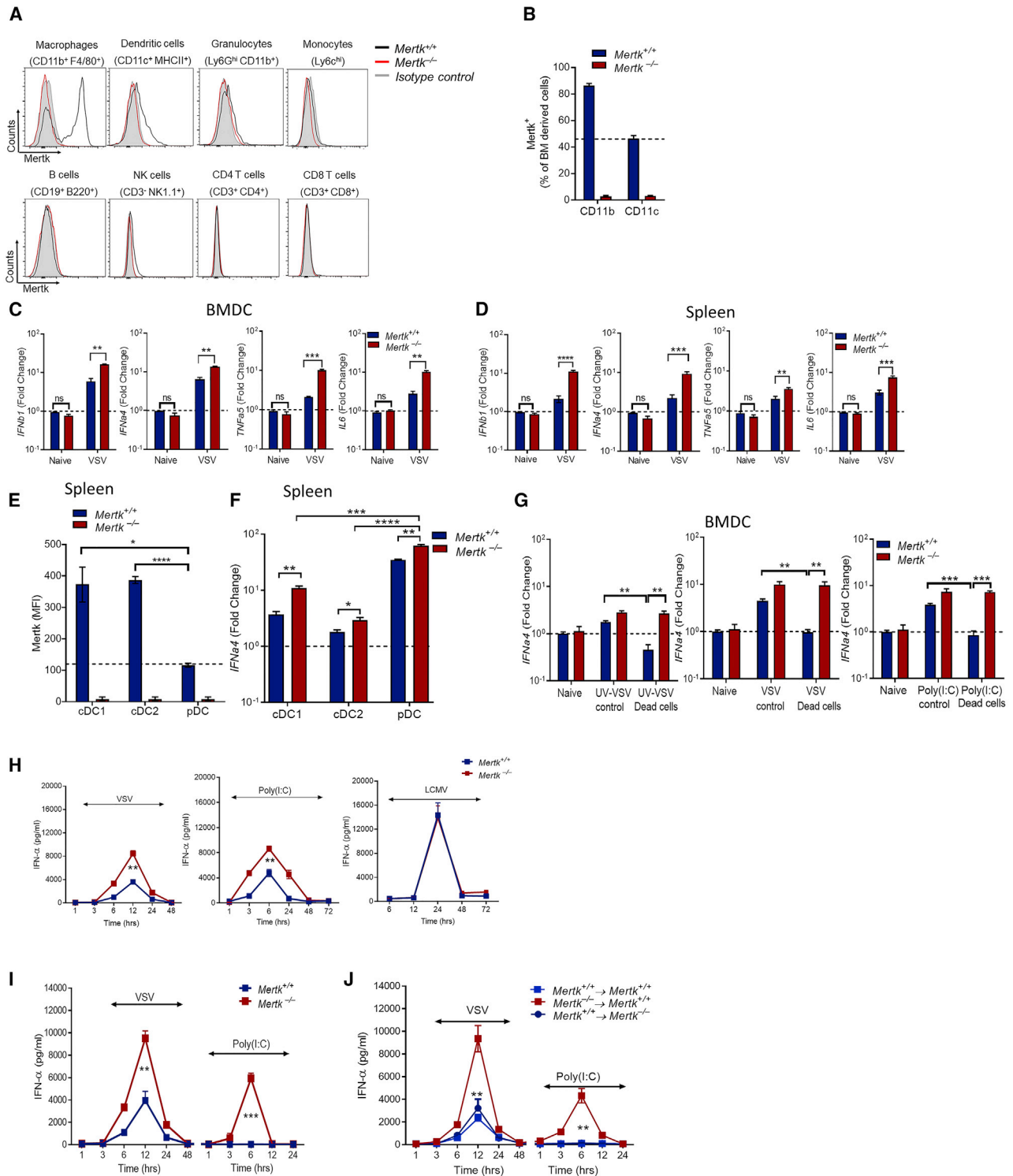
Figure 2. Dead Cells Induce Innate Anergy via Mertk

(A) FACS of Mertk expression on splenic leukocytes of naive Mertk$^{+/+}$ or Mertk$^{-/-}$ mice (n = 5).

(B) FACS of Mertk expression by BM cells of naive Mertk$^{+/+}$ or Mertk$^{-/-}$ mice (n = 3).

(C) IFNa4, IFNb1, TNF-α5, and IL-6 mRNA in BMDCs of Mertk$^{+/+}$ or Mertk$^{-/-}$ that were left naive or infected with VSV (MOI1; 8 h; n = 3).

(D) IFNa4, IFNb1, TNF-α5, and IL-6 mRNA in spleens of Mertk$^{+/+}$ or Mertk$^{-/-}$ mice that were left naive or infected with 2 × 10^8 PFU VSV i.v. (8 h; n = 7).

(E) MFI of Mertk of splenic cDC1, cDC2, and pDCs of naive Mertk$^{+/+}$ or Mertk$^{-/-}$ mice (n = 5).

(legend continued on next page)

Next, we wondered which subset of DCs expressed Mertk. FACS analysis revealed that cDC1 and cDC2 showed higher Mertk expression compared to pDCs (Figure 2E). This correlated inversely with the ability to produce IFN-I, as pDCs sorted from splenocytes of VSV-infected mice showed higher *Ifna4* mRNA when compared to sorted cDC1 and/or cDC2 from the same mice (Figure 2F). Although pDCs were the major producers of IFN-I, there was no obvious cell-type-specific role of Mertk (Figure 2F). We also assayed the mRNA expression levels of both IFN regulatory factor 3 (*Irf3*) and *Irf7*, two positive effectors of IFN signaling during viral infection. We found that the expression of both *Irf3* and *Irf7* was markedly higher in *Mertk*$^{-/-}$ BMDCs and in *Mertk*$^{-/-}$ mice (Figures S2B and S2C), a finding suggesting a generally stronger innate immune activation in *Mertk*$^{-/-}$ mice. These results led us to speculate that the dead cells induced by VSV infection may limit the production of IFN-I via the activation of Mertk signal. To prove that the apoptotic cells dampen IFN-I induction via Mertk, we pretreated BMDCs from *Mertk*$^{+/+}$ and *Mertk*$^{-/-}$ mice with either dead cells or left them untreated and then challenged them with VSV, UV-VSV, or poly (I:C). Dead cells significantly abrogated *Ifna4* induction in *Mertk*$^{+/+}$ BMDCs, but not in *Mertk*$^{-/-}$ BMDCs (Figure 2G). Next, we analyzed the impact of Mertk on the antiviral IFN-I response *in vivo*. In line to our *in vitro* analysis, we found a stronger systemic IFN-I response in *Mertk*$^{-/-}$ mice after challenge with VSV or poly (I:C) (Figure 2H). As lymphocytic choriomeningitis virus (LCMV) is a completely non-cytopathic virus and therefore, in contrast to VSV, does not induce apoptosis in spleens early after infection (Figure S2D), we considered similar levels of IFN-I in WT and *Mertk*$^{-/-}$ mice. In fact, LCMV infection did not show differences in the early IFN-I response (Figure 2H). Next, we verified whether Mertk was indeed the key signal responsible for the IFN-I anergy after VSV infection. We infected *Mertk*$^{+/+}$ and *Mertk*$^{-/-}$ mice with VSV and challenged them after 48 h with poly (I:C). As expected, *Mertk*$^{+/+}$ mice did not produce systemic measurable IFNα upon challenge with poly (I:C) (Figure 2I). In contrast, VSV-infected *Mertk*$^{-/-}$ mice produced systemic IFNα upon challenge with poly (I:C) (Figure 2I). Likewise, when we infected *Mertk*$^{+/+}$ and *Mertk*$^{-/-}$ with VSV and after 48 h challenged them with LCMV, systemically measurable IFNα production was retriggered in *Mertk*$^{-/-}$ mice, but not in *Mertk*$^{+/+}$ mice (Figure S2E). This further proves that indeed dead cells are important for activation of Mertk signals to suppress IFN-I response. To verify that Mertk expressed on hematopoietic cells contributed to innate anergy, we generated BM chimeric mice, where *Mertk*$^{-/-}$ BM was transplanted into irradiated *Mertk*$^{+/+}$ mice. For controls, *Mertk*$^{+/+}$ BM was transplanted into irradiated *Mertk*$^{-/-}$ or *Mertk*$^{+/+}$ mice. Chimeric mice were infected with VSV and challenged after 48 h with poly (I:C). As expected,

Mertk$^{-/-}$ →*Mertk*$^{+/+}$ chimeras showed elevated IFNα production during VSV infection and poly (I:C) challenge (Figure 2J). In contrast, *Mertk*$^{+/+}$→*Mertk*$^{+/+}$ and *Mertk*$^{+/+}$→*Mertk*$^{-/-}$ chimeric mice showed reduced IFN-I levels during VSV infection and no measurable IFN-I after further poly (I:C) treatment (Figure 2J). We concluded that dead cells activate Mertk on DCs, which then induces innate anergy.

Dead Cells Induce IL-10 via Mertk, thereby Dampening the Activation of Innate Immunity

Mertk, as a PS receptor, could be activated by cell debris (Tsou et al., 2014; Kazeros et al., 2008; van der Meer et al., 2014). We therefore proposed that cells, which are lysed by the virus, activate Mertk signals and that this activation induces other inhibitory signals that dampen antiviral responses. Previously, TAM signaling was reported to trigger the expression of SOCS proteins, thereby acting as a "brake" for cytokine production after TLR is activated by pathogens (Yoshimura et al., 2005; Tamiya et al., 2011). Indeed, VSV infection enhanced expression of *SOCS1* and *SOCS3* (Figure 3A). *Mertk*$^{-/-}$ BMDCs showed reduced expression of *SOCS1* and *SOCS3* when compared to WT littermates (Figure 3A). Western blot analysis confirmed that SOCS1 and SOCS3 are induced via Mertk after VSV infection (Figure 3B), which was also confirmed via mRNA expression in spleen of *Mertk*$^{+/+}$ or *Mertk*$^{-/-}$ after VSV infection (Figure 3C). IL-10 is a master regulator of immune response and also regulates the induction of SOCS1 and SOCS3 (Couper et al., 2008; Ding et al., 2003). Besides IL-10, TGF-β is one suppressive cytokine that induces SOCS3 (Ruan et al., 2010; Fox et al., 2003). We hypothesized that IL-10 could play a key role in eliciting immunosuppression during VSV infection. Indeed, we found reduced expression of *IL-10* and *TGF-β* in *Mertk*$^{-/-}$ BMDCs, which were infected with VSV (Figure 3D). To further prove the role of dead cells in inducing IL-10 via Mertk, we pretreated *Mertk*$^{+/+}$ and *Mertk*$^{-/-}$ BMDCs with dead cells and challenged them with VSV, UV-VSV, or poly (I:C). In the presence of dead cells, *Mertk*$^{+/+}$ BMDCs enhanced *IL-10* production in response to VSV, UV-VSV, and poly (I:C) (Figure 3E). In contrast, presence of dead cells showed limited influence on *IL-10* induction in *Mertk*$^{-/-}$ BMDCs (Figure 3E). To determine the impact of DCs on IL-10 and TGF-β production, we sorted splenic DCs from WT mice and compared IL-10 and TGF-β mRNA expressions levels with that in the whole spleen of the same mice after VSV infection. We found DCs were not the major cell types producing these cytokines (Figure S3A). Next, we determined the role of Mertk on IL-10 induction *in vivo*. In line to our *in vitro* data, spleens of *Mertk*$^{-/-}$ mice expressed reduced levels of *IL-10* and *TGF-β* (Figure 3F). Next, we aimed to determine the role of Mertk in inducing IL-10 independent of VSV-induced cell death. Previous

(F) IFNa4 mRNA of sorted splenic cDC1, cDC2, and pDCs of *Mertk*$^{+/+}$ or *Mertk*$^{-/-}$ mice infected with 2 × 10^8 PFU VSV i.v. (8 h; n = 4).
(G) IFNα4 mRNA in BMDCs of *Mertk*$^{+/+}$ or *Mertk*$^{-/-}$ mice that were left naive or pretreated with apoptotic B16F10 cells or media and treated with UV-VSV (MOI1), VSV (MOI1), or poly (I:C) (10 μg/mL; 8 h; n = 3).
(H) IFNα in *Mertk*$^{+/+}$ or *Mertk*$^{-/-}$ mice infected with 2 × 10^8 PFU VSV i.v. (n = 3) or with 2 × 10^6 PFU LCMV WE i.v. (n = 5) or challenged with poly (I:C) i.p. (50 μg per mouse; n = 4).
(I) IFNα in *Mertk*$^{+/+}$ or *Mertk*$^{-/-}$ mice infected with 2 × 10^8 PFU VSV i.v. and, 48 h later, challenged with poly (I:C) i.p. (50 μg per mouse; n = 3).
(J) IFNα in *Mertk*$^{+/+}$→*Mertk*$^{+/+}$, *Mertk*$^{+/+}$→*Mertk*$^{-/-}$, and *Mertk*$^{-/-}$→*Mertk*$^{+/+}$ bone marrow chimeric mice infected with 2 × 10^8 PFU VSV i.v. and, 48 h later, challenged with poly (I:C) i.p. (50 μg/mouse; n = 3). All data are shown as mean +/- SEM. *p < 0.05; **p < 0.01; ***p < 0.001; ****p < 0.0001 (Student's t-test). ns = not significant.
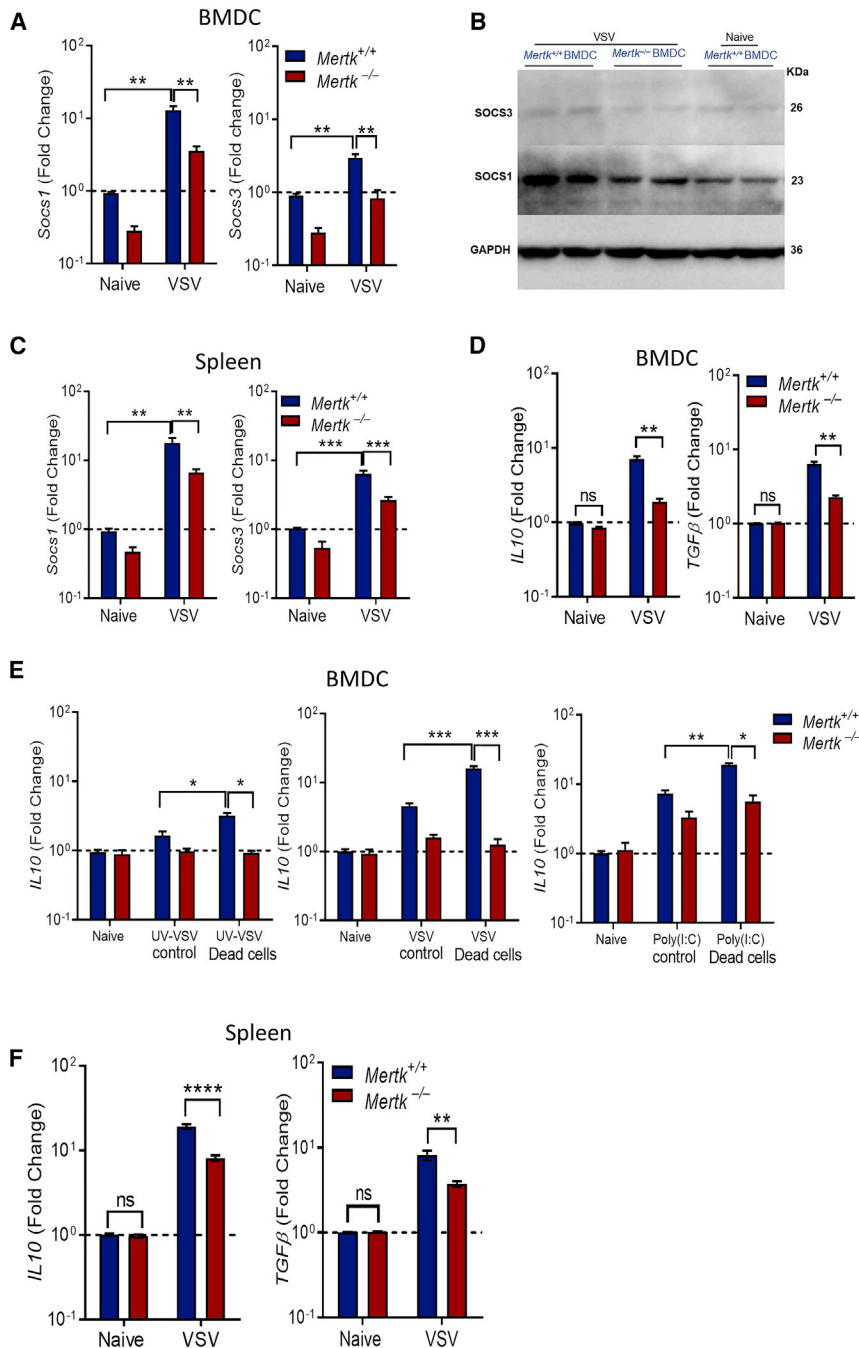
Figure 3. Dead Cells Induce IL-10 via Mertk, thereby Dampening the Activation of Innate Immunity

(A) *SOCS*1 and *SOCS*3 mRNA in BMDCs of *Mertk*$^{+/+}$ or *Mertk*$^{-/-}$ mice that were left naive or infected with VSV (MOI1; 8 h; n = 3).

(B) Representative immunoblots of SOCS1, SOCS3, and GAPDH expression in BMDCs as in (A).

(C) *SOCS*1 and *SOCS*3 mRNA in spleens of naive *Mertk*$^{+/+}$ or *Mertk*$^{-/-}$ mice or mice infected with 2×10^8 PFU VSV i.v. (8 h; n = 7).

(D) *IL-10* and *TGF-β* mRNA in BMDCs of *Mertk*$^{+/+}$ or *Mertk*$^{-/-}$ mice that were left naive or infected with VSV (MOI1; 8 h; n = 3).

(E) *IL-10* mRNA in BMDCs of *Mertk*$^{+/+}$ or *Mertk*$^{-/-}$ mice that were left naive or pretreated with apoptotic B16F10 cells or media and infected with UV-VSV (MOI1), VSV (MOI1), or poly (I:C) (10 µg/mL; n = 3).

(F) *IL-10* and *TGF-β* mRNA in spleens of *Mertk*$^{+/+}$ or *Mertk*$^{-/-}$ mice that were left naive or infected with 2×10^8 PFU VSV i.v. (8 h; n = 7). All data are shown as mean +/- SEM. *p < 0.05; **p < 0.01; ***p < 0.001; ****p < 0.0001 (Student's t-test). ns = not significant.

these findings demonstrate that dead cells induce IL-10 via Mertk, thereby leading to immunosuppression.

Mertk Signaling Limits the Antiviral Immune Response and Virus Control

Next, we anticipated that Mertk deficiency results in efficient antiviral mechanisms, thereby limiting early virus replication. Indeed, *Mertk*$^{-/-}$ mice showed reduced VSV replication in several organs (Figure 4A). Pharmacological inhibition of Mertk similarly reduced virus replication in all organs tested (Figure 4B). These data were in line with *in vitro* cultures of *Mertk*$^{-/-}$ BMDCs (Figure S4A). Interestingly, also within the marginal zone, an area where replication of VSV depends on UBP43 (*Usp18*; Honke et al., 2013), lack or pharmacological inhibition of Mertk limited VSV propagation (Figures S4B and

studies have shown that bile duct and gallbladder ligation (BDL) induces hepatocyte apoptosis (Miyoshi et al., 1999; Sodeman et al., 2000; Faubion et al., 1999). Based on this finding, we induced apoptosis by BDL in *Mertk*$^{+/+}$ and *Mertk*$^{-/-}$ mice and analyzed IL-10. BDL induced active caspase-3 and Mertk expression in livers of WT mice (Figure S3B). Enhanced apoptosis correlated with increased frequencies of IL-10$^+$ DCs and IL-10$^+$ and TGF-β$^+$ macrophages in livers of *Mertk*$^{+/+}$ mice (Figure S3C). Again, IL-10 induction in DCs and macrophages depended on Mertk in the presence of dead cells (Figure S3C). Taken together,

S4C). To rule out that the lower virus titer in *Mertk*$^{-/-}$ mice is not due to differential uptake of virus particle from the circulatory system but rather due to higher production of IFN-I, we determined early virus uptake and IFN-I induction. Clearance of virus inoculum from the blood was comparable between *Mertk*$^{+/+}$ and *Mertk*$^{-/-}$ mice (Figure S4D); however, even after 3 h, *Mertk*$^{-/-}$ mice were already secreting more IFNα (Figure S4E), indicating that the lower virus titer in *Mertk*$^{-/-}$ mice is due to stronger IFN-I response. To get insights how *Mertk*$^{-/-}$ mice could limit VSV propagation, we analyzed IFN-stimulated genes (ISGs), which play a pivotal role

Figure 4. Mertk Signaling Limits the Antiviral Immune Response and Virus Control

(A) Virus titer in organs of $Mertk^{+/+}$ or $Mertk^{-/-}$ mice infected with 2×10^8 PFU VSV i.v. (8 h; n = 4).

(B) Virus titers in organs of WT mice pretreated with either Mertk tyrosine kinase inhibitor (UNC2881) 3 mg/kg or the solvent (DMSO) i.v. on days −3, −2, −1, and 0 and infected with 2×10^8 PFU VSV i.v. (8 h; n = 3).

(C) OAS1, ISG15, and MX1 mRNA in BMDCs of $Mertk^{+/+}$ or $Mertk^{-/-}$ mice that were left naive or infected with VSV (MOI1) (8 h; n = 3).

(D) OAS1, ISG15, and MX1 mRNA in spleens of $Mertk^{+/+}$ or $Mertk^{-/-}$ mice that were left naive or infected with 2×10^8 PFU VSV i.v. (8 h; n = 7).

(E) IL-1β, IL-12, INOS, and CCL5 mRNA in spleens of $Mertk^{+/+}$ or $Mertk^{-/-}$ mice that were left naive or infected with 2×10^8 PFU VSV i.v. (8 h; n = 5).

in mounting an antiviral state within a host cell. *ISG15*, *OAS1*, and *MX1* were highly induced in $Mertk^{-/-}$ BMDCs (Figure 4C) and spleens of $Mertk^{-/-}$ mice (Figure 4D). Besides ISGs, also other inflammatory cytokines or chemoattractants, like *IL-1β*, *IL-12*, *INOS*, and *CCL5*, were highly induced in $Mertk^{-/-}$ mice (Figure 4E), suggesting that not only IFNs and ISGs but also other inflammatory messengers are overexpressed in the absence of Mertk. *Usp18* is a negative regulator of IFN-I signaling and is an important ISG15-specific protease (Malakhova et al., 2003; Honke et al., 2016). Interestingly, absence of Mertk resulted in reduced *Usp18* expression (Figures S4F and S4G). Next, we wondered whether, during VSV infection, the early induction of IL-10 also affects the function of effector T cells. To answer this question, we infected $Mertk^{+/+}$ and $Mertk^{-/-}$ mice with 2×10^6 PFU VSV and analyzed induction of virus-specific T cells by measuring production of IFNγ after *in vitro* restimulation. Lack of Mertk enhances frequencies of virus-specific IFNγ producing CD4+ and CD8+ T cells (Figure 4F). VSV-neutralizing antibody responses were not affected by Mertk (Figure S4H). To gain insights into the overall benefit of Mertk expression during VSV infection, we determined survival after lethal VSV challenge. We found that survival was lower among $Mertk^{+/+}$ mice than $Mertk^{-/-}$ mice (Figure 4G). Taken together, these findings indicate that Mertk mediates immunosuppressive mechanisms during viral infection and thereby limits antiviral responses.

Dexamethasone Dampens Innate Immune Activation via Mertk

Dexamethasone, a synthesized glucocorticoid hormone (GCH), has been shown to upregulate Mertk expression in antigen-presenting cells, whereas proinflammatory signals cause its downregulation (Zizzo et al., 2012; McColl et al., 2009; Keil et al., 1995; Cabezón et al., 2015). Dexamethasone also induces rat thymic apoptosis *in vivo* (Mann and Cidlowski, 2001). Therefore, we proposed that upregulation of Mertk by dexamethasone can limit antiviral mechanisms. To test this theory, we first determined Mertk expression *in vitro* and *in vivo* after dexamethasone challenge. FACS analysis showed that pretreatment of $Mertk^{+/+}$ BMDCs with dexamethasone substantially upregulated Mertk expression (Figure 5A). Similarly, challenge of WT mice with dexamethasone significantly enhanced *Mertk* expression in the spleen and liver (Figure 5B). Next, we investigated the consequences of dexamethasone-induced Mertk overexpression on the innate immune response after acute viral infection. To achieve this, we similarly pretreated $Mertk^{+/+}$ and $Mertk^{-/-}$ mice with or without dexamethasone and infected them with VSV. Interestingly, dexamethasone pretreatment resulted in increased expression of SOCS1 and SOCS3 in $Mertk^{+/+}$ mice, but not in $Mertk^{-/-}$ mice (Figure 5C). In line, mRNA analysis from dexamethasone-pretreated $Mertk^{+/+}$ mice showed a higher

(F) IFNγ+ CD4+ T cells and IFNγ+ CD8+ T cells (%) in splenic and hepatic leukocytes of $Mertk^{+/+}$ or $Mertk^{-/-}$ mice that were left naive or infected with 2×10^8 PFU VSV i.v. (8 days) and then restimulated or left unstimulated (none; n = 3).

(G) Survival of $Mertk^{+/+}$ or $Mertk^{-/-}$ mice infected with 2×10^8 PFU VSV i.v. (n = 6). All data are shown as mean +/- SEM. *p < 0.05; **p < 0.01; ***p < 0.001; ****p < 0.0001 (Student's t-test). ns = not significant.
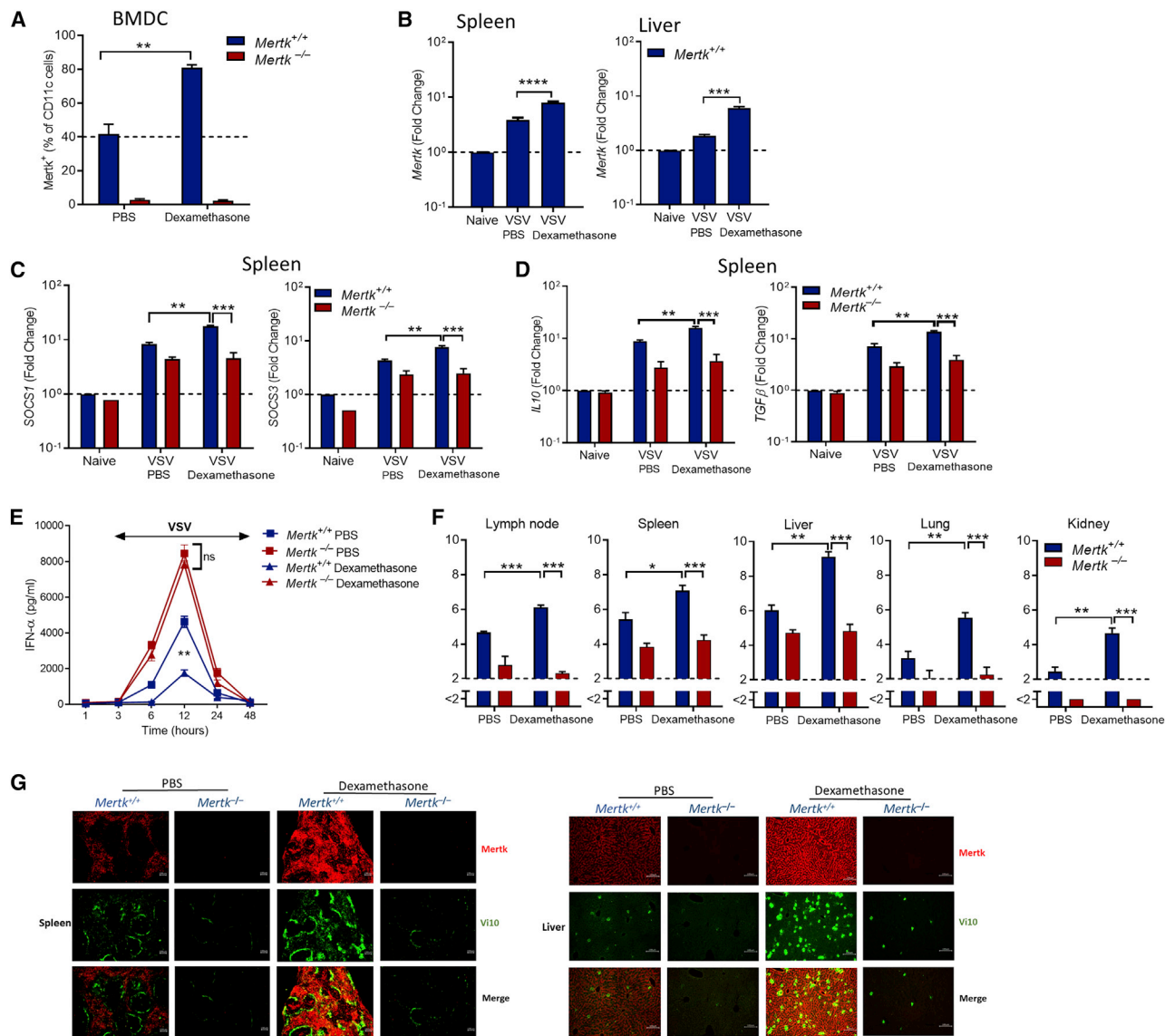
Figure 5. Dexamethasone Dampens Innate Immune Activation via Mertk

(A) FACS of Mertk expression in BMDCs of $Mertk^{+/+}$ or $Mertk^{-/-}$ mice that were treated with dexamethasone (dexa; 4 μM) or PBS (48 h; n = 3).

(B) mRNA expression of *Mertk* in the spleens and livers of $Mertk^{+/+}$ mice that were left naive or pretreated with dexa (50 μg/mouse) or PBS i.p. on days −3, −2, −1, and 0 and infected with 2×10^8 PFU VSV i.v. (8 h; n = 3).

(C and D) SOCS1, SOCS3, IL-10, and TGF-β mRNA levels in the spleens of $Mertk^{+/+}$ or $Mertk^{-/-}$ mice (same condition as in B; 8 h; n = 3).

(E) IFNα in $Mertk^{+/+}$ or $Mertk^{-/-}$ mice (same conditions in B; n = 3).

(F) Virus titers in organs of $Mertk^{+/+}$ or $Mertk^{-/-}$ mice (same conditions as in B; 8 h; n = 3).

(G) Spleens and livers for Mertk (red) and VSV glycoprotein (Vi10; green) of $Mertk^{+/+}$ or $Mertk^{-/-}$ mice (same conditions as in B; 8 h; n = 3). All data are shown as mean +/- SEM. *p < 0.05; **p < 0.01; ***p < 0.001; ****p < 0.0001 (Student's t-test). ns = not significant.

induction of *IL-10* and *TGF-β* when compared to untreated $Mertk^{+/+}$ mice (Figure 5D). This was dependent on Mertk, as $Mertk^{-/-}$ mice showed no comparable difference in *IL-10* and *TGF-β* induction with dexamethasone pretreatment (Figure 5D). Moreover, dexamethasone pretreatment was associated with significantly suppressed serum IFNα levels in $Mertk^{+/+}$ mice, but not in $Mertk^{-/-}$ mice (Figure 5E). Plaque assay data demonstrated disseminated VSV replication in the lymph nodes,

spleens, livers, lungs, and kidneys of dexamethasone-treated $Mertk^{+/+}$ mice, but not dexamethasone-treated $Mertk^{-/-}$ mice (Figure 5F). Likewise, immunofluorescence analysis of the spleen and liver sections from these mice revealed that dexamethasone-induced augmented virus replication depended on Mertk (Figure 5G). These results indicate that Mertk plays a key role in mediating the immunosuppressive effect of dexamethasone.

DISCUSSION

Disease tolerance is broadly defined as the host's ability to limit damage and maintain health when faced with increasing burdens of pathogens and is a general feature of the host responses to infection (Vale et al., 2014). Among the diverse arsenal of defense mechanisms deployed by multicellular hosts are those that rely on rapid induction of apoptosis pathways to trigger premature cell death of infected host cells (Kvansakul, 2017; Handke et al., 2012). Apoptosis has been demonstrated to play a role in a variety of diseases, including viral infections (Razvi and Welsh, 1995). Although rapid clearance of apoptotic cells by phagocytes is important for inhibiting inflammation and autoimmune responses against intracellular antigens, it may also limit antiviral immune responses. Indeed, several studies have found that apoptotic cells exhibit a dramatic immunosuppressive effect *in vivo* (Pittoni and Valesini, 2002; Cohen et al., 2002).

The study reported here found an important interaction between dead cells induced by cytopathic viral infection and the tyrosine kinase receptor Mertk that leads to induction of innate anergy. VSV, an economically significant animal pathogen, is an important inducer of apoptosis. The M protein, a VSV structural component, is responsible for many cytopathic effects in VSV-infected cells, including the inhibition of host gene expression (Lyles, 2000) and the induction of apoptosis (Desforges et al., 2001; Kopecky et al., 2001). The effective immune defense against VSV predominantly involves the antiviral activity of endogenously produced interferon and, subsequently, the generation of neutralizing antibody to the glycoprotein (Lefrancois, 1984; Vandepol et al., 1986). First, we investigated the effect of dead cells on the innate immune response. We found that WT mice previously infected with VSV become unresponsive to IFNα after a challenge with poly (I:C). Indeed, after VSV infection, we detected increased numbers of apoptotic cells using active caspase-3 staining in the spleen. We proposed that the dead cells can induce anergy. We found that the pretreatment of BMDCs harvested from WT mice with dead cells significantly suppressed *IFNα* and enhanced *IL-10* induction after VSV challenge. These findings gave us a hint to suggest that dead cells induced during a cytopathic viral infection are anti-inflammatory and tolerogenic.

The externalization of PS serves as an apoptotic cell recognition signal for multiple phagocytic receptors, including Mertk (Fantl et al., 1993). Therefore, we suggested that Mertk signaling could play a key role in mediating the tolerance induced by dead cells. First, we showed that Mertk is strongly expressed by macrophages and DCs. Determining the relevance of Mertk in antiviral immunity, we found that Mertk deficiency leads to higher IFNα induction in BMDCs and *in vivo* after VSV infection. We concluded that Mertk is one of the key regulators of the innate immune response. Characterizing Mertk expression on DC subsets, we found that Mertk is highly expressed on cDC1 and cDC2 when compared to pDCs, but this correlates inversely with IFNα induction. Because Mertk is a PS sensor on dead cells, we proposed that dead cells can contribute to innate anergy via Mertk. We showed that Mertk-deficient mice previously infected with VSV retriggered IFNα production after challenge with poly (I:C); however, WT mice were unresponsive to

the challenge, as stated previously. Data from Mertk-deficient chimeric mice were in agreement with the above findings. This therefore suggests that the observed innate anergy is dependent on induction of Mertk signals on hematopoietic cells. Inline, the higher *IL-10* and *TGF-β* inductions after VSV challenge are dependent on Mertk. Interestingly, co-culture of dead cells with BMDCs from WT mice significantly suppressed *IFNα* levels and enhanced *IL-10* induction after challenge with UV-VSV, VSV, or poly (I:C). In addition, BDL enhanced apoptotic cell induction in the livers of WT mice, and this was associated with higher IL-10 and TGF-β production in the same organ. SOCS1/3 antagonist peptide was proposed to protect mice against lethal infection with influenza A virus (Ahmed et al., 2015). We demonstrated that lack of Mertk limited *SOCS1* and *SOCS3* induction after VSV challenge. Although the levels of VSV-neutralizing antibody were similar in both WT and Mertk-deficient mice, we suggest that enhanced IFNα production associated with Mertk deficiency is sufficient to allow the mice to survive the infection. Taken together, these findings highlight the crucial role of dead cells in inducing immune homeostasis via Mertk during viral infection.

Dexamethasone is known to induce apoptosis and to upregulate Mertk expression (McColl et al., 2009; Zizzo et al., 2012). Thus, we wondered what influence dexamethasone would exert during viral infection. First, we demonstrated that dexamethasone treatment significantly increases the Mertk expression *in vitro* and *in vivo*. Consequently, pretreatment of WT mice with dexamethasone strongly increased *SOCS1* and *SOCS3* expression after VSV challenge. Inline, IFNα production was significantly diminished in WT mice pretreated with dexamethasone after VSV challenge, and this correlated with highly increased IL-10 and TGF-β induction in these mice. Indeed, dexamethasone pretreatment strongly promoted VSV replication in various organs in a Mertk-dependent manner. Interestingly, these dexamethasone-induced effects were abrogated in the Mertk-deficient mice. These findings strongly indicate that Mertk is an important effector of dexamethasone-induced immunosuppression.

Our results suggest that Mertk-specific inhibitors or blocking antibodies may be a potential class of antiviral therapeutic agents, but the consequences of chronic inflammation induced by these agents must be evaluated. Second, future studies to explore the immunosuppressive role of Mertk in commonly used topically applied stimuli, such as imiquimod, would be interesting. Such findings will broaden our understanding of the crucial role of apoptotic cells in activating Mertk signals not only during viral infection but also in association with autoimmunity and cancer immunology. In summary, dead cells induce tolerogenic state via Mertk. The induction of SOCS1, SOCS3, IL-10, and TGF-β after the activation of Mertk signals extinguishes antiviral mechanisms and results in innate anergy.

STAR★METHODS

Detailed methods are provided in the online version of this paper and include the following:

- KEY RESOURCES TABLE
- LEAD CONTACT AND MATERIALS AVAILABILITY

AUTHOR CONTRIBUTIONS

Conceptualization, T.A., P.A.L., and K.S.L.; Investigation & Analysis, T.A., L.B.C., T.A.H., H.B., V.D., F.L. (Fanghui Li), M.A., E.L., A.H., E.N., V.K., S.-K.F., J.L., J.F.-K., M.B., M.S., Y.M.M., and S.F.; Writing—Original Draft, T.A., P.A.L., and K.S.L.; Writing—Review & Editing, T.A., L.B.C., T.A.H., J.L., F.L., D.H., C.H., P.A.L., and K.S.L.; Resources, C.H., F.L. (Florian Lang), D.H., P.A.L., and K.S.L.; Supervision, P.A.L. and K.S.L.

DECLARATION OF INTERESTS

The authors declare no competing interests.

REFERENCES

A-Gonzalez, N., Bensinger, S.J., Hong, C., Beceiro, S., Bradley, M.N., Zelcer, N., Deniz, J., Ramirez, C., Díaz, M., Gallardo, G., et al. (2009). Apoptotic cells promote their own clearance and immune tolerance through activation of the nuclear receptor LXR. Immunity *31*, 245–258.

Ahmed, C.M., Dabelic, R., Bedoya, S.K., Larkin, J., 3rd, and Johnson, H.M. (2015). A SOCS1/3 antagonist peptide protects mice against lethal infection with influenza A virus. Front. Immunol. *6*, 574.

Barber, G.N. (2005). VSV-tumor selective replication and protein translation. Oncogene *24*, 7710–7719.

Behrens, E.M., Gadue, P., Gong, S.Y., Garrett, S., Stein, P.L., and Cohen, P.L. (2003). The mer receptor tyrosine kinase: expression and function suggest a role in innate immunity. Eur. J. Immunol. *33*, 2160–2167.

Biswas, S.K., and Lopez-Collazo, E. (2009). Endotoxin tolerance: new mechanisms, molecules and clinical significance. Trends Immunol. *30*, 475–487.

Byrne, A., and Reen, D.J. (2002). Lipopolysaccharide induces rapid production of IL-10 by monocytes in the presence of apoptotic neutrophils. J. Immunol. *168*, 1968–1977.

Cabezón, R., Carrera-Silva, E.A., Flórez-Grau, G., Errasti, A.E., Calderón-Gómez, E., Lozano, J.J., España, C., Ricart, E., Panés, J., Rothlin, C.V., and Benítez-Ribas, D. (2015). MERTK as negative regulator of human T cell activation. J. Leukoc. Biol. *97*, 751–760.

Carrera Silva, E.A., Chan, P.Y., Joannas, L., Errasti, A.E., Gagliani, N., Bosurgi, L., Jabbour, M., Perry, A., Smith-Chakmakova, F., Mucida, D., et al. (2013). T cell-derived protein S engages TAM receptor signaling in dendritic cells to control the magnitude of the immune response. Immunity *39*, 160–170.

Chen, W., Frank, M.E., Jin, W., and Wahl, S.M. (2001). TGF-beta released by apoptotic T cells contributes to an immunosuppressive milieu. Immunity *14*, 715–725.

Cohen, P.L., Caricchio, R., Abraham, V., Camenisch, T.D., Jennette, J.C., Roubey, R.A.S., Earp, H.S., Matsushima, G., and Reap, E.A. (2002). Delayed apoptotic cell clearance and lupus-like autoimmunity in mice lacking the c-mer membrane tyrosine kinase. J. Exp. Med. *196*, 135–140.

Couper, K.N., Blount, D.G., and Riley, E.M. (2008). IL-10: the master regulator of immunity to infection. J. Immunol. *180*, 5771–5777.

Desforges, M., Charron, J., Bérard, S., Beausoleil, S., Stojdl, D.F., Despars, G., Laverdière, B., Bell, J.C., Talbot, P.J., Stanners, C.P., and Poliquin, L. (2001). Different host-cell shutoff strategies related to the matrix protein lead to persistence of vesicular stomatitis virus mutants on fibroblast cells. Virus Res. *76*, 87–102.

Ding, Y., Chen, D., Tarcsafalvi, A., Su, R., Qin, L., and Bromberg, J.S. (2003). Suppressor of cytokine signaling 1 inhibits IL-10-mediated immune responses. J. Immunol. *170*, 1383–1391.

Erwig, L.P., and Henson, P.M. (2008). Clearance of apoptotic cells by phagocytes. Cell Death Differ. *15*, 243–250.

Fantl, W.J., Johnson, D.E., and Williams, L.T. (1993). Signalling by receptor tyrosine kinases. Annu. Rev. Biochem. *62*, 453–481.

Faubion, W.A., Guicciardi, M.E., Miyoshi, H., Bronk, S.F., Roberts, P.J., Svingen, P.A., Kaufmann, S.H., and Gores, G.J. (1999). Toxic bile salts induce rodent hepatocyte apoptosis via direct activation of Fas. J. Clin. Invest. *103*, 137–145.

Fox, S.W., Haque, S.J., Lovibond, A.C., and Chambers, T.J. (2003). The possible role of TGF-beta-induced suppressors of cytokine signaling expression in osteoclast/macrophage lineage commitment in vitro. J. Immunol. *170*, 3679–3687.

Fuchs, Y., and Steller, H. (2011). Programmed cell death in animal development and disease. Cell *147*, 742–758.

Gaddy, D.F., and Lyles, D.S. (2005). Vesicular stomatitis viruses expressing wild-type or mutant M proteins activate apoptosis through distinct pathways. J. Virol. *79*, 4170–4179.

Green, D.R., Ferguson, T., Zitvogel, L., and Kroemer, G. (2009). Immunogenic and tolerogenic cell death. Nat. Rev. Immunol. *9*, 353–363.

Hanayama, R., Tanaka, M., Miwa, K., Shinohara, A., Iwamatsu, A., and Nagata, S. (2002). Identification of a factor that links apoptotic cells to phagocytes. Nature *417*, 182–187.

Handke, W., Krause, E., and Brune, W. (2012). Live or let die: manipulation of cellular suicide programs by murine cytomegalovirus. Med. Microbiol. Immunol. *201*, 475–486.

Honke, N., Shaabani, N., Zhang, D.-E., Iliakis, G., Xu, H.C., Häussinger, D., Recher, M., Löhning, M., Lang, P.A., and Lang, K.S. (2013). Usp18 driven enforced viral replication in dendritic cells contributes to break of immunological tolerance in autoimmune diabetes. PLoS Pathog. *9*, e1003650.

Honke, N., Shaabani, N., Zhang, D.-E., Hardt, C., and Lang, K.S. (2016). Multiple functions of USP18. Cell Death Dis. *7*, e2444.

Hunter, A.M., LaCasse, E.C., and Korneluk, R.G. (2007). The inhibitors of apoptosis (IAPs) as cancer targets. Apoptosis *12*, 1543–1568.

Javadi, A., Shamaei, M., Mohammadi Ziazi, L., Pourabdollah, M., Dorudinia, A., Seyedmehdi, S.M., and Karimi, S. (2014). Qualification study of two genomic DNA extraction methods in different clinical samples. Tanaffos *13*, 41–47.

Kaminskyy, V., and Zhivotovsky, B. (2010). To kill or be killed: how viruses interact with the cell death machinery. J. Intern. Med. *267*, 473–482.

Kazeros, A., Harvey, B.G., Carolan, B.J., Vanni, H., Krause, A., and Crystal, R.G. (2008). Overexpression of apoptotic cell removal receptor MERTK in alveolar macrophages of cigarette smokers. Am. J. Respir. Cell Mol. Biol. *39*, 747–757.

Keil, D.E., Luebke, R.W., and Pruett, S.B. (1995). Differences in the effects of dexamethasone on macrophage nitrite production: dependence on exposure regimen (in vivo or in vitro) and activation stimuli. Int. J. Immunopharmacol. *17*, 157–166.

Kopecky, S.A., Willingham, M.C., and Lyles, D.S. (2001). Matrix protein and another viral component contribute to induction of apoptosis in cells infected with vesicular stomatitis virus. J. Virol. *75*, 12169–12181.

Kvansakul, M. (2017). Viral infection and apoptosis. Viruses *9*, E356.

Lefrancois, L. (1984). Protection against lethal viral infection by neutralizing and nonneutralizing monoclonal antibodies: distinct mechanisms of action in vivo. J. Virol. *51*, 208–214.

Lemke, G., and Rothlin, C.V. (2008). Immunobiology of the TAM receptors. Nat. Rev. Immunol. *8*, 327–336.

Lyles, D.S. (2000). Cytopathogenesis and inhibition of host gene expression by RNA viruses. Microbiol. Mol. Biol. Rev. *64*, 709–724.

Malakhova, O.A., Yan, M., Malakhov, M.P., Yuan, Y., Ritchie, K.J., Kim, K.I., Peterson, L.F., Shuai, K., and Zhang, D.E. (2003). Protein ISGylation modulates the JAK-STAT signaling pathway. Genes Dev. *17*, 455–460.

Mann, C.L., and Cidlowski, J.A. (2001). Glucocorticoids regulate plasma membrane potential during rat thymocyte apoptosis in vivo and in vitro. Endocrinology *142*, 421–429.

McColl, A., Bournazos, S., Franz, S., Perretti, M., Morgan, B.P., Haslett, C., and Dransfield, I. (2009). Glucocorticoids induce protein S-dependent phagocytosis of apoptotic neutrophils by human macrophages. J. Immunol. *183*, 2167–2175.

Medvedev, A.E., Sabroe, I., Hasday, J.D., and Vogel, S.N. (2006). Tolerance to microbial TLR ligands: molecular mechanisms and relevance to disease. J. Endotoxin Res. *12*, 133–150.

Miyoshi, H., Rust, C., Roberts, P.J., Burgart, L.J., and Gores, G.J. (1999). Hepatocyte apoptosis after bile duct ligation in the mouse involves Fas. Gastroenterology *117*, 669–677.

Nakano, T., Ishimoto, Y., Kishino, J., Umeda, M., Inoue, K., Nagata, K., Ohashi, K., Mizuno, K., and Arita, H. (1997). Cell adhesion to phosphatidylserine mediated by a product of growth arrest-specific gene 6. J. Biol. Chem. *272*, 29411–29414.

Nassar, M., Tabib, Y., Capucha, T., Mizraji, G., Nir, T., Pevsner-Fischer, M., Zilberman-Schapira, G., Heyman, O., Nussbaum, G., Bercovier, H., et al. (2017). GAS6 is a key homeostatic immunological regulator of host-commensal interactions in the oral mucosa. Proc. Natl. Acad. Sci. USA *114*, E337–E346.

Pittoni, V., and Valesini, G. (2002). The clearance of apoptotic cells: implications for autoimmunity. Autoimmun. Rev. *1*, 154–161.

Razvi, E.S., and Welsh, R.M. (1995). Apoptosis in viral infections. Adv. Virus Res. *45*, 1–60.

Rose, J.K., and Whitt, M.A. (2001). Rhabdoviridae: the viruses and their replication. ScienceOpen.

Rothlin, C.V., Ghosh, S., Zuniga, E.I., Oldstone, M.B.A., and Lemke, G. (2007). TAM receptors are pleiotropic inhibitors of the innate immune response. Cell *131*, 1124–1136.

Roulston, A., Marcellus, R.C., and Branton, P.E. (1999). Viruses and apoptosis. Annu. Rev. Microbiol. *53*, 577–628.

Ruan, M., Pederson, L., Bradley, E.W., Bamberger, A.M., and Oursler, M.J. (2010). Transforming growth factor-beta coordinately induces suppressor of cytokine signaling 3 and leukemia inhibitory factor to suppress osteoclast apoptosis. Endocrinology *151*, 1713–1722.

Seitz, H.M., Camenisch, T.D., Lemke, G., Earp, H.S., and Matsushima, G.K. (2007). Macrophages and dendritic cells use different Axl/Mertk/Tyro3 receptors in clearance of apoptotic cells. J. Immunol. *178*, 5635–5642.

Sodeman, T., Bronk, S.F., Roberts, P.J., Miyoshi, H., and Gores, G.J. (2000). Bile salts mediate hepatocyte apoptosis by increasing cell surface trafficking of Fas. Am. J. Physiol. Gastrointest. Liver Physiol. *278*, G992–G999.

Svensson, M., Maroof, A., Ato, M., and Kaye, P.M. (2004). Stromal cells direct local differentiation of regulatory dendritic cells. Immunity *21*, 805–816.

Tamiya, T., Kashiwagi, I., Takahashi, R., Yasukawa, H., and Yoshimura, A. (2011). Suppressors of cytokine signaling (SOCS) proteins and JAK/STAT pathways: regulation of T-cell inflammation by SOCS1 and SOCS3. Arterioscler. Thromb. Vasc. Biol. *31*, 980–985.

Taylor, R.C., Cullen, S.P., and Martin, S.J. (2008). Apoptosis: controlled demolition at the cellular level. Nat. Rev. Mol. Cell Biol. *9*, 231–241.

Tsou, W.-I., Nguyen, K.-Q.N., Calarese, D.A., Garforth, S.J., Antes, A.L., Smirnov, S.V., Almo, S.C., Birge, R.B., and Kotenko, S.V. (2014). Receptor tyrosine kinases, TYRO3, AXL, and MER, demonstrate distinct patterns and complex regulation of ligand-induced activation. J. Biol. Chem. *289*, 25750–25763.

Vale, P.F., Fenton, A., and Brown, S.P. (2014). Limiting damage during infection: lessons from infection tolerance for novel therapeutics. PLoS Biol. *12*, e1001769.

van der Meer, J.H., van der Poll, T., and van 't Veer, C. (2014). TAM receptors, Gas6, and protein S: roles in inflammation and hemostasis. Blood *123*, 2460–2469.

Vandepol, S.B., Lefrancois, L., and Holland, J.J. (1986). Sequences of the major antibody binding epitopes of the Indiana serotype of vesicular stomatitis virus. Virology *148*, 312–325.

Verma, A., Warner, S.L., Vankayalapati, H., Bearss, D.J., and Sharma, S. (2011). Targeting Axl and Mer kinases in cancer. Mol. Cancer Ther. *10*, 1763–1773.

Voll, R.E., Herrmann, M., Roth, E.A., Stach, C., Kalden, J.R., and Girkontaite, I. (1997). Immunosuppressive effects of apoptotic cells. Nature *390*, 350–351.

Wakkach, A., Fournier, N., Brun, V., Breittmayer, J.-P., Cottrez, F., and Groux, H. (2003). Characterization of dendritic cells that induce tolerance and T regulatory 1 cell differentiation in vivo. Immunity *18*, 605–617.

Wallet, M.A., Sen, P., Flores, R.R., Wang, Y., Yi, Z., Huang, Y., Mathews, C.E., Earp, H.S., Matsushima, G., Wang, B., and Tisch, R. (2008). MerTK is required for apoptotic cell-induced T cell tolerance. J. Exp. Med. *205*, 219–232.

Yoshimura, A., Nishinakamura, H., Matsumura, Y., and Hanada, T. (2005). Negative regulation of cytokine signaling and immune responses by SOCS proteins. Arthritis Res. Ther. *7*, 100–110.

Zhang, W.J., and Zheng, S.S. (2005). In vitro study of immunosuppressive effect of apoptotic cells. J. Zhejiang Univ. Sci. B *6*, 919–925.

Zhang, M., Tang, H., Guo, Z., An, H., Zhu, X., Song, W., Guo, J., Huang, X., Chen, T., Wang, J., and Cao, X. (2004). Splenic stroma drives mature dendritic cells to differentiate into regulatory dendritic cells. Nat. Immunol. *5*, 1124–1133.

Zizzo, G., Hilliard, B.A., Monestier, M., and Cohen, P.L. (2012). Efficient clearance of early apoptotic cells by human macrophages requires M2c polarization and MerTK induction. J. Immunol. *189*, 3508–3520.

STAR★METHODS

KEY RESOURCES TABLE

REAGENT or RESOURCE	SOURCE	IDENTIFIER
Antibodies		
Anti-Mertk	eBioscience	Cat # 17-5751-82; RRID: AB_2716943
NK1.1	Biolegend	Cat #108707; RRID: AB_313394
Anti-CD3	abcam	Cat # ab91493; RRID: AB_2049420
Anti-CD4	eBioscience	Cat # 17-0041-82; RRID: AB_469320
Anti-CD8	eBioscience	Cat # 25-0081-82; RRID: AB_469584
Anti- CD11b	BD Bioscience	Cat # 11-0112-81; RRID: AB_464935
Anti- CD11c	eBioscience	Cat # 25-0114-82; RRID: AB_469590
Anti- CD11c	eBioscience	Cat # 17-0114-82
anti-CD19	eBioscience	Cat # 15-0193-82; RRID: AB_469346
Anti45R (B220)	eBioscience	Cat #45-0452-82; RRID: AB_1107006
anti-CD317	eBioscience	Cat #12-3179-42; RRID: AB_10596640
anti-Ly6C	eBioscience	Cat # 45-5932-82; RRID: AB_2723343
anti-Ly6G	eBioscience	Cat # 15-5931-82; RRID: AB_468813
Anti- F4/80	eBioscience	Cat # 17-4801-82; RRID: AB_2784648
7-AAD	Biolegend	Cat # 420403
Annexin	Biolegend	Cat # 640908
Anti-CD169	eBioscience	Cat # 12-5755-82; RRID: AB_2572625
Anti-CD45.2	eBioscience	Cat # 12-0454-82; RRID: AB_465678
Anti-active Caspase-3	BD Bioscience	Cat # 559341; RRID: AB_397234
Anti- IL-10	eBioscience	Cat # 12-7101-82; RRID: AB_466176
Anti-TGF-β	Novus biologicals	Cat # IC240G-100UG
Anti-VSV-GP (Vi10)	Self made	In-house
SOCS1	Cell Signaling	Cat # 3950S; RRID: AB_2192983
SOCS3	Cell Signaling	Cat # 52113S; RRID: AB_2799408
Bacterial and Virus Strains		
VSV virus stock	Originally obtained from Prof. F. Lehmann-Grube, Heinrich Pette Institute, Hamburg, Germany).	N/A
LCMV WE	LCMV-WE was originally obtained from F. Lehmann-Grube (Heinrich Pette Institute, Hamburg, Germany) and was propagated on L929 cells (obtained from ATCC, NCTC clone 929).	N/A
Chemicals, Peptides, and Recombinant Proteins		
VSV-P52 peptide	PolyPeptide Laboratories, Strasbourg, France	N/A
VSV-P8 peptide	PolyPeptide Laboratories, Strasbourg, France	N/A
Mer tyrosine kinase inhibitor (UNC2881)	Selleckchem	Cat # S7325
Dexamethasone	mibe-GmbH, Brehna, Germany	Cat # PZN-08704344.
Experimental Models: Cell Lines		
MC57 cells	obtained from Ontario Cancer Institute, Canada	N/A
Vero cells	ATCC	N/A
B16F10 cells	ATCC	N/A
Experimental Models: Organisms/Strains		
C57BL/6J mice	Jackson Laboratories	JAX000664
Mertk$^{-/-}$ Mice	Jackson Laboratories	Stock No. 011122

(Continued on next page)

REAGENT or RESOURCE	SOURCE	IDENTIFIER
Myd88/Trif/Cardif⁻/⁻ Mice	Jackson Laboratories	Cross-bred locally at the animal facility
Ifnar⁻/⁻ Mice	Jackson Laboratories	32045-JAX
Software and Algorithms		
FlowJo software	FlowJo LLC, Ashland, OR, USA	N/A
Graphpad prism	Graphpad software inc. California corporation, San Diego, USA	N/A
Other		
Fluorescence Microscope HS BZ-9000 series (BIOREVO)	Keyence, Osaka, Japan	N/A
FLUOstar Omega ELISA Reader	BMG Labtech, Ortenberg Germany	N/A
ChemiDoc MP Imaging system	BioRad, California, USA	N/A
Cryostat CM 3050S	Leica, USA	N/A
LightCycler 480 realtime PCR machine	Roche, Basel, Switzerland	N/A
FACS Fortessa (BD)	Becton Dickinson, New Jersey, USA	N/A

LEAD CONTACT AND MATERIALS AVAILABILITY

This study did not generate new unique reagents. Further information and request for resources should be directed to and will be fulfilled by the Lead Contact, Tom Adomati (wennatom@yahoo.com).

EXPERIMENTAL MODEL AND SUBJECT DETAILS

Ethics statement

Animal experiments were authorized by the State Agency for Nature, Environmental and Consumer Protection of North Rhine-West-phalia (Landesamt für Natur, Umwelt und Verbraucherschutz Nordrhein-Westfalen) and were conducted in accordance with the German laws for animal protection or according to institutional guidelines at the Ontario Cancer Institute of the University of Toronto Health Network.

Mice

Mertk⁻/⁻ mice were bred heterozygously onto a C57BL/6 (B6) background (backcrossed at least 5 times). F5 (5th generation from backcross with B6) *Mertk⁻/⁻* mice were directly compared with littermate controls (*Mertk⁺/⁺* mice). *Ifnar⁻/⁻* and *Myd88/Trif/ Cardif⁻/⁻* mice were maintained on B6 background. All animals were housed in single ventilated cages. Male and female mice were used for all studies. Mice were between 7-10 weeks of age. During survival experiments, the health status of the mice was checked twice daily. After the appearance of clinical signs of VSV replication in the central nervous system, such as paralysis, mice were removed from the experiment and were considered dead.

Genotyping by PCR

The *tail lysis buffer* containing proteinase K was used to digest the tail samples overnight. DNA was extracted by the phenol/chlo-roform method (Javadi et al., 2014) . The following oligonucleotide primers that detect murine Mertk were used: 1) Mertk⁺/⁺ primer, 5′ -TTC TTG TTC TGG GGT TGA CTC-3′; 2) common sense primer, 5′-CAT CTG GGT TCC AAA GGC TA-3′, a common sense primer that detects both sequences; and 3) Mertk⁻/⁻ primer, 5′-ATC AGC AGA CTC TGT TCC AC-3′ (all from biomers.net, Ulm/Donau, Germany). The product was analyzed on 2% agarose gels in Tris-borate-ethylenediaminetetraacetic acid (EDTA) buffer and visualized by ethidium bromide staining.

Bile duct and gallbladder ligation (BDL)

Animals were anesthetized by isoflurane and placed on a heating pad. After intubation and ventilation, the animals were shaved and the skin disinfected. A midline incision in the upper abdomen was made; the common bile duct and the gallbladder were identified, isolated, and ligated with 6–0 coated vicryl Polyglactin fiber from Ethicon (Johnson & Johnson Medical GmbH, Norderstedt, Germany). The fascia and skin of the midline abdominal incision were closed with 5–0 vicryl Polyglactin fiber from Ethicon (Johnson & Johnson Medical GmbH, Norderstedt, Germany). Sham treatment was performed similarly but without ligation of the bile duct and gallbladder. Animals were monitored for 3 days during recovery and analyzed.

Bone marrow chimeras

For generation of bone marrow chimeras, *Mertk⁺/⁺* mice and *Mertk⁻/⁻* mice were irradiated with a single dose of 9.5Gy from X-ray source in one fraction. After 24 h, mice were reconstituted intravenously with 10×10^6 bone marrow cells from either *Mertk⁺/⁺* or *Mertk⁻/⁻* mice. Mice were analyzed 30 days after reconstitution.

METHOD DETAILS

Specific Mer tyrosine kinase inhibitor (UNC2881)

Mer tyrosine kinase inhibitor was purchased from Selleckchem.com (Catalog No.S7325; Munich, Germany). It was diluted in dimethyl sulfoxide (DMSO; 50 mg/ml) and then administered intravenously at a dose of 3 mg/kg on day 3 before infection (d-3), d-2, and d-1.

Treatment with Dexamethasone (PZN-08704344)

Dexamethasone (dexa) was purchased from JenaPharm with stock concentration of 4mg ml^{-1}, (Catalog No.PZN-08704344; mibe-GmbH, Brehna, Germany). It was diluted in phosphate buffered saline (PBS) and then administered intraperitoneally at a dose of 50 μg/100μl before infection on day 3 (d-3), d-2, and d-1. For *in vitro* experiments, DCs were treated with 4μM dexamethasone 48 h before analysis.

Generation of BMDCs and BMDMs

Primary DCs or macrophages were generated by isolating bone marrow cells from femurs and tibias of mice, followed by the elimination of erythrocytes. Bone marrow cells were cultured in very low endotoxin-DMEM (Biochrom) supplemented with 10% (v v^{-1}) lipopolysaccharide (LPS)-free FCS (Biochrom); 1% (v v^{-1}) penicillin-streptomycin-glutamine (ThermoFisher Scientific); 0.1% (v v^{-1}) 50mM β-mercaptoethanol (β-ME) (Invitrogen); and 3% (v v^{-1}) granulocyte–macrophage colony-stimulating factor (DCs) (made in-house from X63 cell line) or 20% (v v^{-1}) monocyte colony stimulating factor (macrophages) (made in-house from L929 cell line). On day 6 after harvesting, cells were washed with Dulbecco's phosphate-buffered saline (DPBS), and 5×10^6 cells were cultured in 10ml Petri dish or 2×10^5 cells were plated in 24 well plate for 2 more days. For dexamethasone experiment, on day 6 after harvesting, the BMDCs were treated with dexamethasone (4μg ml^{-1}, Jenapharm) for further 48 h.

Generation of apoptotic B16F10 cells

B6-derived melanoma cell line (B16F10) cells were cultured in 10% FCS in Dulbecco's modified Eagle's medium (DMEM; PAN-Biotech, Aidenbach, Germany) in the presence of puromycin (0.03 μg/ml) for 3 days. The cells were heat-stressed in a water bath at 50°C for 15 min and then incubated at 37°C for an additional 12 h.

Virus and plaque assays

VSV, Indiana strain (VSV-IND, Mudd-Summers isolate), was originally obtained from Professor D. Kolakofsky (University of Geneva, Switzerland). Virus was propagated on BHK-21 cells at a multiplicity of infection (MOI) of 0.01. The VSV concentration was determined as described below and was then plaque-purified on Vero cells. Mice were infected intravenously with various doses of VSV. Virus titers were measured with a plaque-forming assay. For this assay, organs were crushed in DMEM containing 2% FCS, titrated 1:3 over 12 steps, and plaqued onto Vero cells. After a 2 h incubation at 37°C, an overlay was added, and the virus preparation was again incubated at 37°C. Plaques were counted 24 h later after crystal violet staining.

Neutralizing antibody assay

Serum was prediluted with 2% FCS DMEM (1:40). The complement system was inactivated at 56°C for 30 min. For analysis of total immunoglobulin (Ig; IgM and IgG) kinetics, serum was titrated 1:2 over 12 steps and was incubated with 500 PFU VSV. After incubation for 90 min at 37°C, the virus–serum mixture was plaqued onto Vero cells. An overlay was added after 1 h, and the mixture was incubated again for 24 h at 37°C. Plaques were counted by crystal violet staining. Antibody titers were presented as two- or three-fold dilution steps ($\log_2$ and $\log_3$) times the predilution factor (that is, x40).

Histology

Histologic analyses of snap-frozen tissue were performed with a monoclonal antibody to VSV glycoprotein (Vi10; made in-house). Anti- F4/80 (BM8), Anti-CD169 (SER-4), Anti-Mertk (DSSMMER), anti-CD45.2 (104), and active anti–caspase-3 (C92-605) monoclonal antibodies were purchased from eBioscience (Waltham, MA, USA). Sections for caspase-3 staining were washed and stained with streptavidin (eBioscience). In brief, sections were fixed with acetone, and nonspecific antigens were blocked for 10 min in PBS containing 2% FCS or for 1 h in PBS containing 10% FCS (anti–caspase-3). They were then stained for various antibodies and diluted 1:100 in blocking solution for 1 h (Vi10, Anti-F4/80, Anti-CD169, anti-CD45.2 and Anti-Mertk) or 2 h (anti-active caspase-3). Images of stained sections were acquired with a fluorescence microscope (BZ-II analyzer; KEYENCE, Osaka, Japan).

Flow cytometry

Spleens were dissociated in FACS buffer, and splenocytes were incubated with anti-NK1.(PK136) (biolegend, Koblenz, Germany), anti-CD(H146-968) from abcam, anti-Mertk (DSSMMER), anti-CD4 (GK1.5), anti-CD8 (52-6.7), anti-CD11b (M1/70), anti-CD11c (N418), anti-CD19 (1D3), anti-CD45R(B220) (RA3-6B2), anti-Ly6C (HK1.4), anti-Ly6G (RB6-8C5), anti-MHCII (M5/114.15.2), anti-F4/80 (BM8) all from eBioscience (Waltham, MA, USA). Bone marrow derived cells were extracted and cultured as shown previously and surface stained with anti-Mertk (DSSMMER), anti-CD11b (M1/70), anti-CD11c (N418) all from eBioscience (Waltham, MA, USA). After 6 h of re-stimulation with VSV antigen p8 peptide or p52 peptide, lymphocytes were stained with anti-CD8 (52-6.7), anti-CD4

(GK1.5), and anti–IFNγ (XMG1.2) all from eBioscience (Waltham, MA, USA). For measurement of intracellular IFNγ, cells were fixed with formaldehyde (2% formaldehyde solution in phosphate-buffered saline, PBS) for 10 min, permeabilized with saponin (1%) solution, and stained with anti–IFNγ (XMG 1.1) antibody from eBioscience. Live or dead cells were stained with annexinV (PI; eBioscience) and 7-AAD (biolegend, Koblenz, Germany) for 30 min at room temperature. For measurement of intracellular IL-10, and TGF-β production on macrophages and DCs cells were stained with surface antibodies such as anti-CD11b (M1/70), anti-CD11c (N418) and anti-F4/80 (BM8) all from eBioscience (Waltham, MA, USA). The cells were then fixed with formaldehyde (2% formaldehyde solution in PBS) for 10 min, permeabilized with saponin (1%) solution, and stained with anti- IL-10 (JES5-16ES) or TGF-β (9016) antibodies (from eBioscience and Novus biologicals respectively). For profiling Mertk expression on sorted DC sub population, the splenocytes were stained as follows; cDC1 (anti-CD11c [N418] and anti-CD8 [52-6.7] all from eBioscience); cDC2 (anti-CD11c [N418] from eBioscience and anti-CD11b [M1/70] from BD bioscience); pDC (anti-B220 [RA3-6B2], anti-CD11c [N418], and anti-CD317 [26F8] all from eBioscience); anti- Mertk (from eBioscience) antibodies. All antibodies were diluted 1:100 to their original concentration in FACS buffer. All stained cells were analyzed on either an LSRII or an FACS LSRFortessa flow cytometer (BD Biosciences), and data were analyzed with FlowJo software (Ashland, OR, USA).

Sorting of DC subpopulation
Spleen of naive and infected mice were digested to obtain splenocytes. 1ml of *Ammonium-Chloride*-Potassium (ACK) buffer was added to each pellet for 2mins to lyse erythrocytes and then washed with 1:20 dilution of MACS buffer containing PH-7.2 phosphate buffered saline (PBS), 0.5% bovine serum albumin (BSA) and 2Mm EDTA. Anti-CD16/32, anti-CD19, -CD3e, -Ly6G and –NK1.1 antibodies were added for 10 mins at 4°C. Pellet were washed and anti-Biotin microbeads solution was added and incubated for 10 mins at 4°C and then washed. Anti-CD11c, -CD8a, -CD11b, -B220 and PDCA1 antibodies for FACS sorting was added for 10 mins at 4°C, after incubation cells were washed with PBS and then proceed for sorting.

Immunoblotting
DCs were cultured for 7days in a medium containing 3% (v v^{-1}) granulocyte–macrophage colony-stimulating factor and then infected with VSV at an MOI of 1. After 8 h, the cells were lysed with boiling sodium dodecyl sulfate (SDS) buffer (1.1% SDS, 11% glycerol, 0.1 M Tris; pH 6.8) containing 10% 2-mercaptoethanol. Total cell extracts were examined with 10% SDS polyacrylamide gel electrophoresis (SDS-PAGE) gels and transferred onto Whatman nitrocellulose membrane (GE Healthcare, Chicago, IL, USA) by standard techniques. Membranes were blocked for 1 h in 5% milk (non-fat dried milk) (PAA Laboratories, Etobicoke, ON, CAN) in PBS supplemented with 0.1% Tween 20 (PBS-T) and were incubated with the primary antibodies anti-SOCS1 (A156) and anti-SOCS3 (D6E1T) (both from Cell Signaling Technology, Danvers, MA, USA). The secondary antibodies rabbit anti-mouse IgG (gamma. ch. Sp; Invitrogen, Carlsbad, CA, USA) and anti–glyceraldehyde 3-phosphate dehydrogenase (anti-GAPDH; Meridian Life Science, Memphis, TN, USA) were detected by horseradish peroxidase (HRP)-conjugated anti-mouse IgG (Bio-Rad Laboratories, Hercules, CA, USA) antibody, anti-rabbit IgG (GE Healthcare) antibody, or both. Signals were detected with the ChemiDoc imaging system (Bio-Rad) and analyzed with the manufacturer's software. Images were cropped for presentation.

RT-PCR
Total RNA was extracted from spleen, liver, and DCs with TRIzol reagent (Ambion, Foster City, CA, USA) according to the manufacturer's instructions. RNA was transcribed with a QuantiTect Reverse Transcription Kit (QIAGEN, Hilden, Germany). Quantitative RT-PCR amplification of single genes was performed with SYBR Green quantitative PCR master mix in a Light Cycler 480 (Roche, Indianapolis, IN, USA). QuantiTect Primer assays for IFNα4, IFNβ1, TNFα, IL-6, SOCS1, SOCS3, IL-10, TGFβ, and Mertk (QIAGEN) were used for quantification of mRNA expression by the respective genes. For analysis, expression levels of target genes were normalized to GAPDH, 18S ribosomal RNA (QIAGEN), or both as an internal control gene (ΔCt). Gene expression values were then calculated with the ΔΔCt method. Relative quantities (RQs) were determined with the equation RQ¼ = $2^{-\Delta\Delta Ct}$.

Enzyme-linked immunosorbent assay measurements
For detection of IFNα in murine serum, we used 96-well flat-bottom microwell plates coated with monoclonal antibody to mouse IFNα (eBioscience). The microwell strips were washed twice and then incubated with sample and biotin conjugate at room temperature for 2 h. Plates were washed with washing buffer and incubated with HRP-conjugated anti-mouse IgG antibody (eBioscience) for 60 min. Plates were washed and incubated with 1X tetramethylbenzidine (TMB) substrate solution (eBioscience) in the dark for 30 min, after which 10% H_2SO_4 solution was added to stop the color reaction. Optical density was measured at 450 nm (FLUOstar Omega microplate reader, BMG LABTECH, Offenberg, Germany).

QUANTIFICATION AND STATISTICAL ANALYSIS

Statistical analyses were performed using GraphPad Prism version 8 (GraphPad Software). Data are expressed as mean ± standard error of the mean (SEM). Student's t test was used to detect statistically significant differences between groups. Significant

differences between several groups were detected by one-way analysis of variance (ANOVA) with Bonferroni or Dunnett post hoc tests. Survival was compared with log-rank (Mantel-Cox) tests. The level of statistical significance was set as $*p < 0.05$; $**p < 0.01$; $***p < 0.001$; $****p < 0.0001$, ns = not significant.

DATA AND CODE AVAILABILITY

This study did not generate or analyze datasets and/or code.